Scientific Papers of the University of Pardubice,
Series A; Faculty of Chemical Technology
24 (2018) 167–185.

University
of Pardubice
Faculty
of Chemical Technology

Band ratio model for remote estimating the water quality parameters in small inland water bodies based on Landsat ETM+ data

Kwasi Asare Baffour Danquah and Tomáš Brunclík*

Institute of Environmental and Chemical Engineering,
The University of Pardubice, CZ–532 10 Pardubice, Czech Republic

Received: May 29, 2018; Accepted: June 28, 2018

This work tries to explore how the remote sensing could be used in monitoring of selected water quality (WQ) parameters in small inland water bodies. The respective models to estimate the water quality parameters were proposed based on the Landsat 7 ETM+ images taken in 6 samplings from May 2012 to September 2014. The images used were scenes of WRS-2, path and row 191/25, as well as 190/25, respectively. Samples were taken from 13 water bodies, from which 9 water bodies (20–90 Ha) were used in modelling (and some removed due to clouds and imagery gaps). The WQ parameters were chlorophyll-a (Chl-a), Total Carbon (TC), Total Organic Carbon (TOC), Total Nitrogen (TN), Temperature (T), and Secchi Disk Depth (SDD). The 3 × 3 moving average-window technique with a water-only-mask approach was used in order to limit the process toward the water areas only. The best models based on the surface reflectance (T based on brightness temperature [K]) showed a correlation r^2 between 0.78 and 0.90 and NRMSE between 16.6 % and 8.0 %, respectively, for all the water quality indicators. This has proved that all the parameters can be remotely estimated. The models and workflow scheme created are intended to help to institutions mandated in the monitoring of water bodies.

Keywords: Landsat; Remote sensing; Algorithms; Model; Water quality; Water monitoring

Introduction

Water bodies, such as lakes and ponds, need to be carefully managed, as the water quality has a significant effect on the humans, aquatic organisms, and upon the

* Corresponding author, ✉ Tomas.Brunclik@upce.cz

environment in general. The term "inland water" as described by Mishra [1] can be used for any ecosystem unless specifically termed otherwise. The deterioration of the water quality of inland water bodies is a serious ecological and social problem, since many lakes, ponds, reservoirs, and other inland water bodies (both natural and artificial) are the main sources of drinking water or are used for recreation and fishery. Inland water bodies in the Czech Republic are not different. To ensure a standard quality for the individual water bodies, it is a tedious and costly task [2]. Measuring of the respective quality parameters has to be done *in-situ* and the samples taken to the laboratory for analysis, which is both labour intensive and time consuming [3].

Remote sensing based methods for the water quality monitoring is one way of addressing the constraints that comes with such measurements. For this purpose, special algorithms are used for remotely sensed data to characterize the water quality, when various researchers utilize different satellite sensors for such monitoring of the respective parameters [4–8]. There are numerous sensors that can be used in remote sensing, such as LANDSAT, MODIS, MERIS, VIIRS, and HySpIRI [9]. By using these sensors, it is possible to measure the colour of water in detail and the variables — i.e., water quality parameters —, such as chlorophyll-a (Chl-a), total suspended sediment, coloured dissolved matter, and Secchi disk depth (SDD), can then be all observed quantitatively [10]. To do so, various studies have come up with algorithms based on Landsat data for estimating the individual types of water quality variables being monitored [11–19]. Such algorithms comprise the single bands, band ratios or other band combinations based on empirical relationship between the blue 450–500 nm, green 500–600 nm, and red 600–700 nm bands to remotely estimate the levels of chlorophyll-a in the inland water bodies.

For instance, Brezonik [16] found the best correlation with a simple band ratio algorithm having used the bands 1 and 3 of Landsat TM with r^2 over 0.88,

$$\ln\left(Chl\text{-}a\right) = -1.7237\,x + 9.6487 \tag{1}$$

where x is a ratio of bands 1/3 and when an addition of yet another variable besides the band1/band3 ratio had not brought significant improvement.

In this study, we chose the Landsat ETM+ imagery taking into account the spatial, temporal, and spectral resolution of the available imagery. Due to the size of the water bodies being monitored, a better spatial resolution compared to MODIS, MERIS, OCM-2, etc. has prevailed, as that supported also by Malthus and his report [10].

The following reasons were also in favour of choosing the Landsat ETM+:

- economic reasons (available for free),
- easy and quick access to Landsat data from United States Geological Survey (USGS),
- extended scope (coverage),
- availability of the already processed images.

In this paper, we seek to

- use the remote sensing as a tool to estimate the water quality parameters in small inland water bodies in the Pardubice and Hradec Kralove regions by constructing a model based on multiple water bodies, as well as multiple sampling using the Landsat ETM+ data,
- effect of 3 × 3 window averaging on the data used,
- the effect of atmospheric correction on the data used.

All the water bodies sampled during this research are relatively small compared to water bodies, which are object of modelling in most of the mentioned articles. One of the objectives is thus also a finding if satellite monitoring using 30 m Landsat data is applicable to such small water bodies. The Landsat 7 was the only Landsat satellite available from the beginning of the sampling and its long operational time allows us to use the models created to estimate the water quality parameters from 1999 to the present and, thanks to a close similarity of TM and ETM+ sensor bands, it would be possible to go even further back in time, but this is out of scope of this article. A newer Landsat 8 and especially Sentinel-2 satellites are superior to Landsat 7 with respect to the sensor spatial and spectral resolution, when the water quality models for such sensors are also prepared.

Along with commonly modelled Chl-a and SDD, we also tried to estimate total organic carbon (TOC), total nitrogen (TN), and temperature (T) using the same methodology. In the case of TOC, the main reason was to explore how well this water quality parameter would agree with satellite models compared to Chl-a, because of an easier measurement, together with the occurrence of chlorophyll-a indicating the overall eutrophication of water and its pollution. Total organic carbon in water is a result of mixture of both dissolved and suspended organic matter present in water, only part of which causes the water colouring and changes in its transparency detectable by the satellite. In our opinion, it is not so different from the case of the chlorophyll-a parameter as it may seem at a first glance. While chlorophyll-a is a green substance, the optical properties of water are affected by many other substances, some of them being optically similar, namely chlorophylls -b, -c, and the products of chlorophyll decomposition as such. In principle, in the case of Chl-a, we are estimating a subset of what the satellite can really "see" and, vice versa, for TOC. In both cases, we can estimate this parameter thanks to an inter-correlation in occurrence of the involved substances.

The total carbon (TC) parameter was added to evaluate its correlation as well, because it is measured along with TOC in the same laboratory instrument, although we are aware that the substantial inorganic carbon component in this parameter has likely little to do with the water quality or colour registered by the satellite. TN is another parameter measured easily by the same analytical instrument, and nitrogen is both part of biomass and a nutrient, so it might also correlate with the algae content and eutrophication, as well as with the satellite bands. Temperature is usually estimated by computing the brightness of temperature from the satellite thermal bands [20,21]. In this work, we tried to apply the same regression-based algorithm on the computed band of the brightness temperature like that for the reflexive satellite bands of the other water quality parameters.

Materials and methods

Study area

This work concentrates on water bodies near Pardubice (50°02′19″N 15°46′45″E) and Hradec Kralove (50°12′34″N15°50′00″E), two larger towns in Eastern Bohemia. Water bodies in the selected area are mainly fishponds and reservoirs formed after sand mining (Fig. 1).

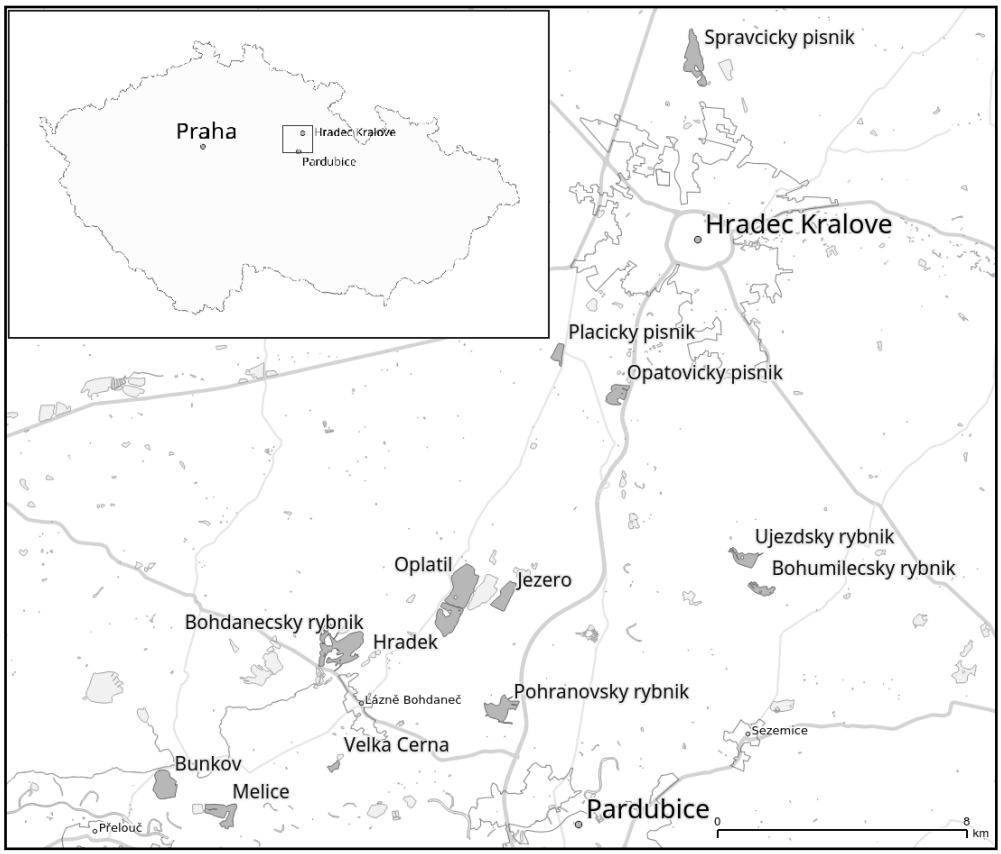

Fig. 1 *Study area*

In the map, the water bodies sampled are highlighted by deeper grey colour, but the other water bodies visible can be monitored via the models as well.

All the water bodies are relatively small, those sampled in this work range from 8 to 90 hectares, approximately. The fish ponds were established in middle ages [22] and have inflow and outflow. Water reservoirs originating from sand mining are relatively new, on some of the water bodies the mining stopped few years ago, and do not have their own inflow / outflow. Most of water bodies of both types are used for fishing and water sports. In most of the fishponds, there is more or less intensive fish breeding / feeding.

In situ sampling and laboratory analysis

The samples were collected from the autumn of 2011 to spring of 2015. Field measurements took place on all 13 inland water bodies (highlighted in Fig. 1). GPS unit Trimble Juno SB was used to record the coordinates of these sites and the track of the boat used. Samples were taken using an inflatable boat and stored in cooling box with ice to ensure cold and dark conditions. One and a half litres of each of the water body was collected from a surface horizon of about 10 cm beneath the waterline. The sampling was done anytime in various water bodies between morning and afternoon, on the day of the satellite overpass, or if not possible, one day in advance or after the overpass. The respective temperatures were read out using a digital thermometer and Secchi disc depth (SDD) recorded at the time of sampling using 20 cm diameter Secchi disk. The water bodies for sampling namely are: Bohdanecsky rybnik*, Bohumilecsky rybnik, Bunkov,* Hradek*, Jezero, Melice, Opatovicky pisnik, Oplatil, Placicky pisnik, Pohranovsky rybnik,* Spravcicky pisnik*, Ujezdsky rybnik,* Velka Cerna. Due to the satellite data quality check (see next chapter), not all sampled water bodies and measurements were used for model development. Those actually used are highlighted using italic font in the above list, i.e. the mentioned water area ranging from 20 to 90 hectares. The weather conditions during sampling times were quite calm with some intermittent cloudy conditions. Nevertheless, visibility (general atmospheric clarity) on all the water bodies at the time of sampling was good.

Some researchers have suggested that ground data collection should be done preferably in parallel with Landsat data acquisition, which helps to minimize errors when calibrating algorithms [16,23,24]. Other researchers state that measurements made 10 days after or before satellite overpass are acceptable as reported in [2] or that *in-situ* measurements taken a day before or after overpass tend to bring tightest correlation but a larger area to cover with longer revisit time may bring some loss in correlation [25]. *In-situ* measurements in this paper were thus mostly taken on the day of the satellite overpass. Where not possible, it was done a day before or a day after.

The chlorophyll-a analysis was done in the laboratory according to ISO-10260 [26], using Fisher micro fibre glass filters with 0.7 μm pore size. The pigment extraction process was accomplished by grinding the filter in ethanol (90%, v/v). The extract was hot water bathed at 75 °C for 5 min. and afterwards allowed to cool down for 15 min. before being put in a refrigerator for another minimal 30 min. This ensured a sufficient concentration of the chlorophyll-a for spectrophotometric determination.

Total carbon (TC), Total organic carbon (TOC) and Total nitrogen (TN) analyses were done using a TOC/TN device and directly from collected samples. Table 1 summarises all the *in-situ* measurements. Not all of the individual samples and measurements were finally used in the model proposal, as part of them was later removed based on visual quality control of the satellite data in the location of measurement points (described in the next chapter in Fig. 2 and its caption). The empty cells mean no measurement of the particular water quality parameter was done.

Table 1 *In situ measurements, mean and standard deviation*

Date	Samples	*Chl-a*	*TC* [mg L^{-1}]	*TOC* [mg L^{-1}]	*TN* [mg L^{-1}]	*T* [°C]	Secchi [cm]
2011.09.15	9	1.5–71				19.5–20.9	
2011.09.26	9	0.2–29					
2012.05.29	9	2.2–31.9	53.3–58.9	16.0–18.1	0.16–0.18	21.0–23.4	21–480
2012.06.22	4	2.9–36.3	34.2–71.5	8.5–21.3	0.10–0.16	24.2–26.3	62–186
2012.07.31–08.01	8	0.7–9.7				26.3–28.4	44–228
2012.09.18	3	3.0–68.9	31.2–84.1	6.1–30.6	0.10–0.19	19.5–22.2	15–220
2012.11.14	6	2.2–8.0		4.2–6.9		8.3–9.2	240–635
2013.04.23	6	3.9–7.3	38.2–43.2	4.5–9.5	0.11–0.15	11.5–13.8	123–184
2013.05.09	4	0.4–20.9	35.0–60.8	6–19.1	0.31–1.68	18.7–22.7	52–620
2013.06.19	10	0.2–65.7	39.2–72.2	7.7–34.8	0.36–3.19	25.1–29.9	19–364
2013.07.29	9	0.5–49.5	26.8–99.5	5.4–43.9	0.36–3.52	26.6–29.9	22–485
2013.08.12	8	0.4–4.7	26.8–45.5	4.6–12.2	0.50–1.23	24.7–52.2	65–499
2014.05.21	8	0.7–8.1	31.0–52.8	8.2–15.0	0.62–1.40	18.8–21.6	125–275
2014.07.23	7	0.2–34.9	35.7–95.6	6.4–42.2	0.59–3.35	24.6–25.8	23–325
2014.09.16	6	1.9–39.1	34.0–85.2	5.8–31.0	0.59–2.54	20.3–21.0	24–490
2015.04.21	8	5.1–35.6	34.5–46.2	7.1–15.5	0.78–1.57	11.9–15.1	66–255
Mean		12.42	48.12	13.82	0.94	21.65	207.3
Std Dev		16.53	19.18	10.10	0.85	6.08	168.0

Satellite data, processing, and smoothing

Images from Landsat 7 ETM+ with a spatial resolution of 30 by 30 m were used. The study area is fully covered by both Landsat scenes of WRS-2, path and row 191/25 and 190/25 respectively, having an average satellite revisit time of 8 days. The corresponding images were downloaded from Earth Explorer (see http://earthexplorer.usgs.gov). We analysed together data from the individual sampling dates. The problem of missing data strips in Landsat 7 imagery [27] was solved by removing affected measurements from the processing, if the measurement location is not covered by smoothing filter described further on.

Cloud cover and cloud shade sometimes impacted the satellite images used for analysis. To identify such areas affected by haze and thin clouds, we used the RGB band combination as suggested in literature (see [24]). The band combination 1,6,6 (L1 Blue 0.450–0.515 nm, L6 Thermal Infrared 10.40–12.50 nm) (Fig. 2) was used to highlight the areas affected by haze and clouds. Such an approach is relative, showing which areas of an image are relatively more or less hazy. Thus, we checked this also by using true colour imagery with a fixed colour interpretation, which was used to check all the images. Based on this, all the measurements that fell into the affected areas were completely removed.

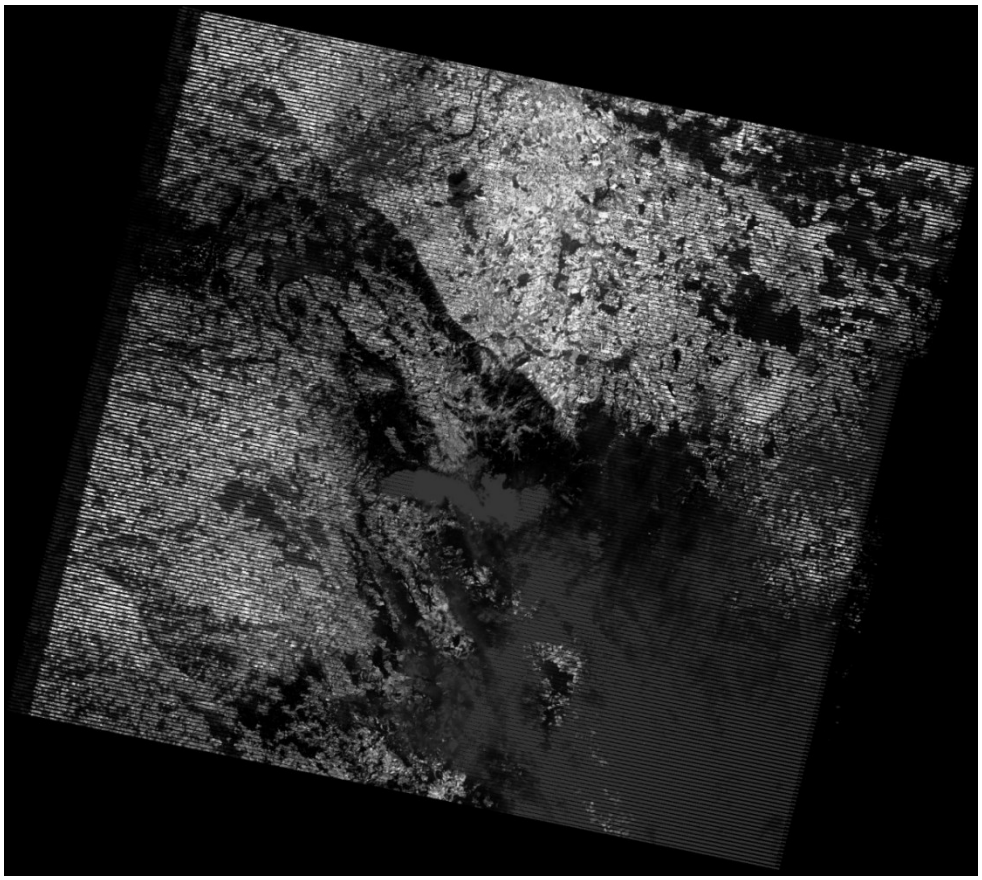

Fig. 2 *RGB band combination 1,6,6 on example of Landsat 7 image path/row 190/25, acquisition date 2011.09.25*

Various levels of the satellite data processing were tried in the initially developed models. The digital number (DN) pixel values obtained from Landsat 7 ETM+ were converted into TOA (top of atmosphere) reflectance. Along with DN data, also surface reflectance (SR) product by USGS (http://earthexplorer.usgs.gov) was downloaded and used. An assumption that atmospherically corrected SR product should perform best for reflective bands was confirmed; therefore, in this particular work, atmospherically corrected images were used.

Band 6 of ETM+ (10400–12500 nm) is the thermal infrared band being used to create the temperature model. DN's were converted into brightness temperature in Kelvins, since this band is not available as atmospherically corrected [28]. The brightness temperature computed from the band 6 corresponds to the temperature measured in situ precisely only for the surfaces having properties of the absolutely black body. Moreover, it is affected by the influence of atmosphere above the surface. Because of these facts, the brightness temperature may differ from the actual temperature measured on the water surface. It was not used directly as the result, but as input into a regression model described in next chapter.

To reduce the negative impact of noise in the imagery on the models, image smoothing was used on reflective bands. A water-only-mask was created based on a detailed vector map of inland water bodies in the Czech Republic (map data © VÚV TGM, http://www.dibavod.cz) and infrared bands thresholding. The mask limited the area for which the averaging 3 × 3 window was used. Through smoothing the noise effect was limited and non-water areas, such as vegetation along the banks of the water bodies, were eliminated. By using the 3 × 3 averaging window, the images were spatially filtered by convolving the image with a small window. Each pixel in the original image was replaced by a weighted average of the product from the window, which applies also to the neighbouring pixels [29],

$$DN_{\text{new}} = \sum_{i=1}^{9} Z_{\text{i}} DN_{\text{i}_{\text{orig}}} DN \tag{2}$$

where the *DN* represents the brightness values of the pixels and Z_{i} is divisor that equals to the inverted number of values in the averaging window matrix (herein, $Z_{\text{i}} = 1/9$). The same formula applies to DN, TOA, and SR imagery.

In order to achieve the above described, the following steps were included:

Step 1 Using r.mask command in Grass GIS, a mask was created based on existing detailed water areas map. Non water areas were masked out.

Step 2 Using map calculator in Grass GIS, an open water mask was created based on band 7 threshold (Band7 < 210). This way water areas affected by water vegetation, the surface algae cover, accumulated sediment, etc. were masked out (in addition to the mask created in step 1).

Step 3 Using the r.mfilter in Grass GIS a filter was ran to smooth the open water pixel values using the 3 × 3 average window.

Effectively, the high and low values are averaged out by reducing the extreme values, eliminating possible artificial or unusual correlations that might arise from noise in the imagery [30]. In the same time, by computing the average in floating point numbers, the smoothing process increases the actual number of digital levels in the band, having effectively increased radiometric resolution at the cost of decreasing intrinsic spatial resolution – although actual pixel size is not changed, discernible high frequency details are reduced. This detail reduction should not have any adverse effect on the model since water-quality parameter levels usually do not exhibit high-frequency spatial changes.

Development of models

The monitoring of the various inland water vis-à-vis, the various parameters under consideration are defined based on the changes in optical properties of the water column [30,31]. By selecting the spectral bands and band ratios (band combinations) for consideration in creating the models for the various parameters, all possible reflective band combinations were first evaluated based on linear r^2 between the respective parameter and every band combination.

In case of temperature, considering, that at least part of the differences between measured and brightness temperature should have character of the additive and multiplicative factor in the space of actual vs. brightness temperature, we then treated the brightness temperature in the same way as the other bands, constructing the linear regression model between the values of brightness temperature and the respective measurements.

Three indices used in assessing the performance of the models developed were the coefficient of determination (r^2), the root mean square error (RMSE), and normalized root mean square error (NRMSE) serving in assessment of the models that had been created based on measured vs. estimated values. Based on these indices and on closeness of a model to the 1:1 line in the performance charts, the best model for each water quality parameter could be chosen. Such a model can then be applied to the satellite imagery in order to obtain the maps of the water quality at the water surfaces visible in the imagery as described below.

Results and discussion

Spectral bands selected for model creation and analysis

Table 2 shows all the coefficients r^2 whose values are 0.6 and above that considered after plotting the actual measurement of parameters against the smoothed values extracted from Landsat 7 ETM+ image spectral bands. In the table, one can see that all the water quality parameters (except temperature T)

were in general correlations with the Landsat 7 ETM+ band 3 (L3 onwards) and band combinations (ratios) of L1 (0.450–0.515 nm), L2 (0.520–0.605 nm), L3 (0.630–0.690 nm). This also shows that combination of the Landsat 7 ETM+ band L1 (0.450–0.515 nm) and band L3 (0.630–0.690 nm) was probably the most suitable for the Chl-a modelling, as well as for SDD, TC and TOC, because of best correlations. Here, it should be noted that higher correlations of logarithm of a parameter with bands not always mean a better resulting model (as shown later on) and so linear and logarithmic correlations should not be directly compared. TN shows a better correlation with combination of bands L2 and L1.

Table 2 *Bands and band combinations considered for model creation*

Parameter	Band	r^2	Parameter	Band	r^2
SDD	L1/L2	0.64	TOC	L1/L2	0.62
SDD	L1/L3	0.77	TOC	L1/L3	0.75
SDD	L2/L1	0.69	TOC	L2/L1	0.78
SDD	L3/L1	0.75	TOC	L3/L1	0.90
Log(*SDD*)	L3	0.71	Log(*TOC*)	L2	0.71
Log(*SDD*)	L1/L2	0.61	Log(*TOC*)	L3	0.64
Log(*SDD*)	L1/L3	0.80	Log(*TOC*)	L1/L2	0.73
Log(*SDD*)	L2/L1	0.74	Log(*TOC*)	L1/L3	0.76
Log(*SDD*)	L3/L1	0.90	Log(*TOC*)	L2/L1	0.81
Chl-a	L1/L3	0.61	Log(*TOC*)	L3/L1	0.85
Chl-a	L2/L1	0.64	TN	L2/L1	0.75
Chl-a	L3/L1	0.80	TN	L3/L1	0.68
Log(*Chl-a*)	L3	0.77	TN	L4/L1	0.60
Log(*Chl-a*)	L1/L3	0.86	Log(*TN*)	L1/L2	0.70
Log(*Chl-a*)	L2/L3	0.74	Log(*TN*)	L2/L1	0.79
Log(*Chl-a*)	L3/L1	0.80	T	L1	0.88
Log(*Chl-a*)	L3/L2	0.74	T	L61	0.87
TC	L2	0.67	T	L62	0.88
TC	L3	0.74	T	L1/L61	0.89
TC	L1/L3	0.75	T	L1/L62	0.89
TC	L2/L1	0.62	T	L61/L1	0.90
TC	L3/L1	0.83	T	L62/L1	0.90
Log(*TC*)	L2	0.66	Log*T*	L1	0.91
Log(*TC*)	L3	0.73	Log*T*	L61	0.84
Log(*TC*)	L1/L3	0.77	Log*T*	L62	0.86
Log(*TC*)	L2/L1	0.63	Log*T*	L1/L61	0.92
Log(*TC*)	L3/L1	0.84	Log*T*	L1/L62	0.92
TOC	L2	0.71	Log*T*	L61/L1	0.87
TOC	L3	0.69	Log*T*	L62/L1	0.87

This also buttressed the point that the bands in the visible region of the spectrum are most suitable for Chl-a and SDD analysis as found in most literature sources mentioned in the Introduction.

Analysis for Temperature (*T*) was done based on uncorrected imagery because atmospherically corrected images of Landsat ETM+ (CDR-Surface Reflectance Climate Data Record, http://earthexplorer.usgs.gov) has no longer thermal infrared bands. Among all the parameters, the temperature had the best linear correlation of up to 0.92 between the measured values and a band or band combination values; specifically, with thermal bands L61 and L62 and surprisingly also with the blue band L1.

Model creation and validation

After analysing correlations of the various bands in relation to the parameters being monitored, different regression models vis-à-vis the *in-situ* measurements were constructed. To measure the performance of these models, we checked r^2, RMSE, NRMSE for each of the model created and those with appreciably strong levels of all three indices considered. Table 3 shows the best two models for each water quality parameter and their properties. The range means minimum and maximum measured value of the parameter used in model development, *n* is the number of individual measurements used in the model development.

Table 3 *Best two models for every water quality parameter*

Parameter	Models	r^2	RMSE	NRMSE	Range (min–max)	*n*
SDD [cm]	245.7 × (L1/L3) – 194.4	0.77	102	16.6 %	19–635	32
SDD [cm]	10^(–1.819 × (L3/L1) + 3.347)	0.77	105	17.1 %	19–635	32
Chl-a [μg L^{-1}]	33.66 × (L3/L1)^3.405	0.82	8.4	12.8 %	0.2–65.7	30
Chl-a [μg L^{-1}]	10^(–0.8330 × (L1/L3) + 2.331)	0.82	8.5	12.9 %	0.2–65.7	30
TC [mg L^{-1}]	53.946 × (L3/L1) + 15.150	0.83	7.5	13.2 %	29.1– 85.2	25
TC [mg L^{-1}]	10^(–0.1640 × (L1/L3) + 1.988)	0.81	8.1	14.3 %	29.1– 85.2	25
TOC [mg L^{-1}]	33.58 × (L3/L1) – 6.0159	0.90	3.5	11.5 %	4.2–34.8	25
TOC [mg L^{-1}]	10^(0.9279 × (L3/L1) + 0.4906)	0.87	4.2	13.5 %	4.2–34.8	25
TN [mg L^{-1}]	10^(1.764 × (L2/L1) – 2.051)	0.78	0.47	15.2 %	0.09–3.19	25
TN [mg L^{-1}]	3.257 × (L2/L1) – 2.294	0.75	0.49	16.0 %	0.09–3.19	25
T [°C]	0.0154 × (L62/L1) – 27.05	0.90	1.7	8.0 %	8.3–29.9	36
T [°C]	1.1203 × L62 – 302.78	0.88	1.9	8.8 %	8.3–29.9	36

The predictive models were used to estimate various parameters and then model performance charts made, showing a relation between the estimates and the *in-situ* measurements. Fig. 3 illustrates such charts for the best model for every water quality parameter. Similar charts could be assembled for several models of each water quality parameter and best model chosen based on the model parameters r^2, RMSE, NRMSE and the charts.

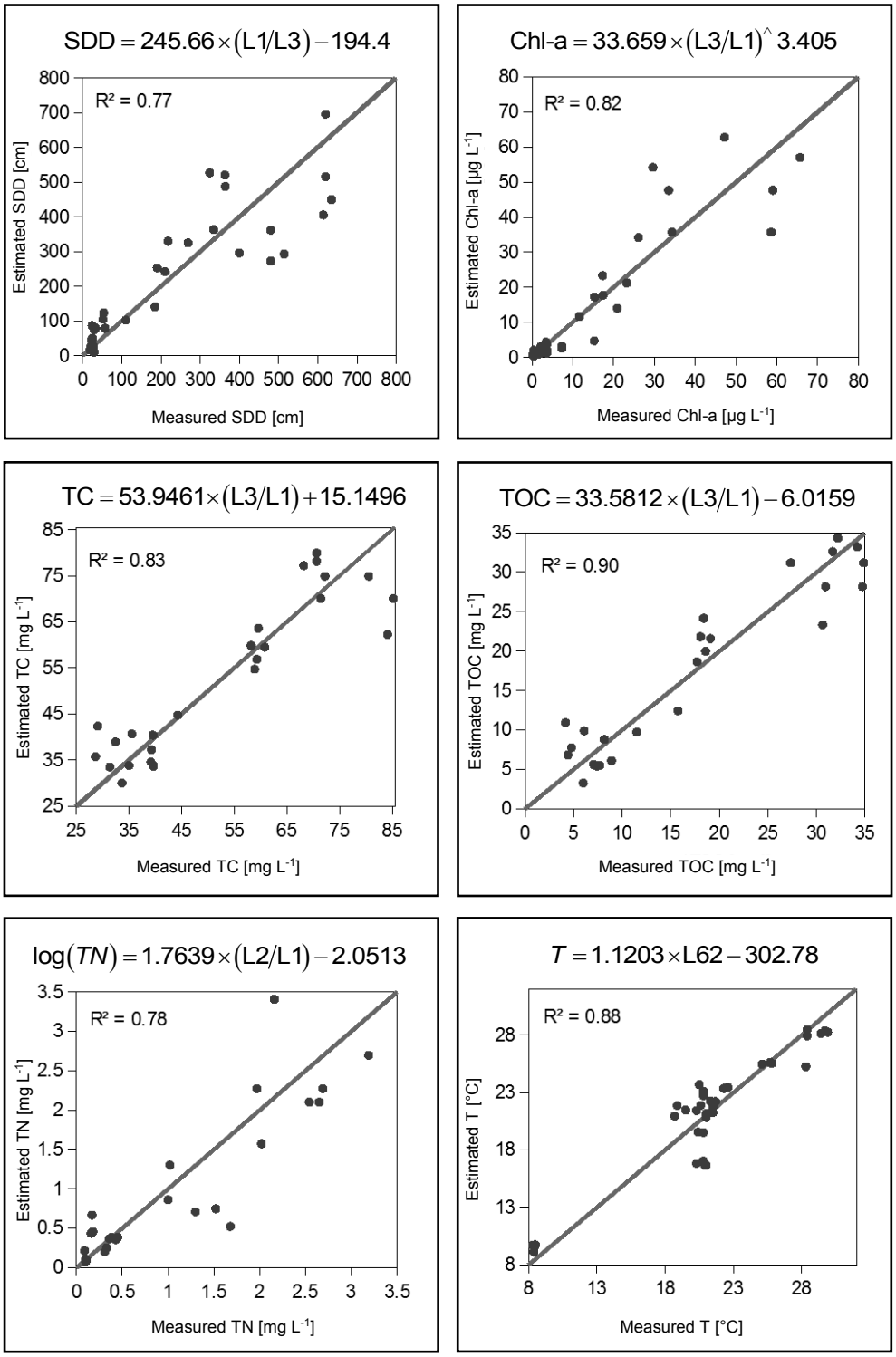

Fig. 3 *Performance of best models created for the various parameters 6.33 cm*

Chlorophyll-a model application

A set of Figs. 4, 5, 6, 7, 8, and 9 surveys the levels of chlorophyll-a and its spatial distribution on the surface of Oplatil, Bohdanecsky rybnik and the surrounding water reservoirs during the year 2012, namely from May to November (compare with Fig. 1 to identify the water bodies by shape). The estimated levels of Chl-a were based on the model:

$$Chl\text{-}a = 33.6\left(\frac{L3}{L1}\right)^{3.405} \tag{3}$$

Bohdanecsky rybnik is a protected national reserve serving as a breeding habitat for numerous species of wild birds. Based on models that have been developed, various water-quality parameters of such water bodies could be estimated without disturbing the habitat of these birds.

The average levels of Chl-a for Bohdanecsky rybnik and Oplatil were computed with the aid of the model as the average Chl-a concentration over the area of the water body visible in the image. This was to estimate time line of Chl-a for the two water bodies, showing an example of how to properly apply the model. It should be noted that Chl-a levels could be estimated also for all the smaller water objects visible in the map. The average for Oplatil and Bohdanecsky rybnik for 29th of May 2012 was 3.5 μg L^{-1} and 33.6 μg L^{-1}, respectively (Fig. 4). For the 23nd of June the average concentrations of Chl-a were 4.9 μg L^{-1}, 64.4 μg L^{-1} per model (Fig. 5).

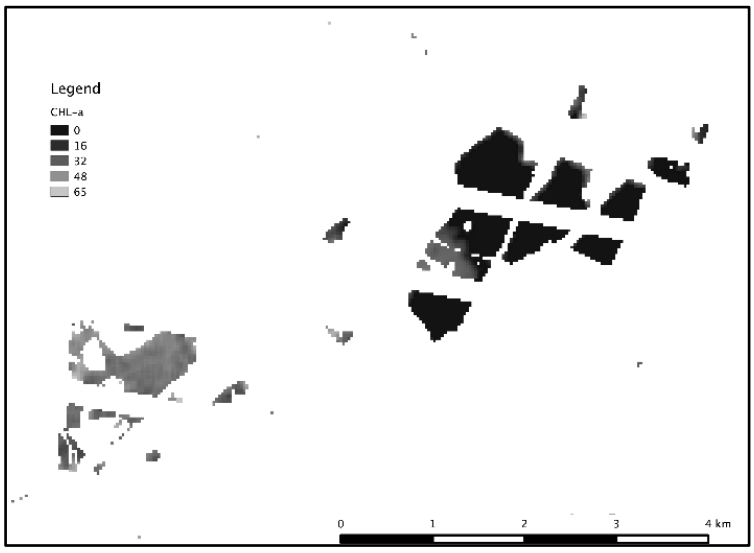

Fig. 4 *Chl-a on Oplatil and Bohdanecsky rybnik on 2012.05.29*

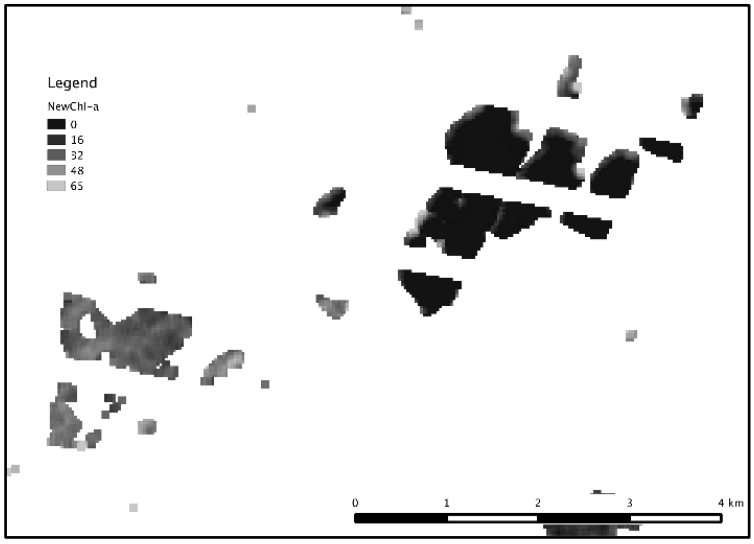

Fig. 5 *Chl-a on Oplatil and Bohdanecsky rybnik on 2012.06.23*

The next date (August 1st, 2012) showed 4.1 μg L^{-1}, 52.4 μg L^{-1} (Fig. 6) for Oplatil and Bohdanecsky rybnik.

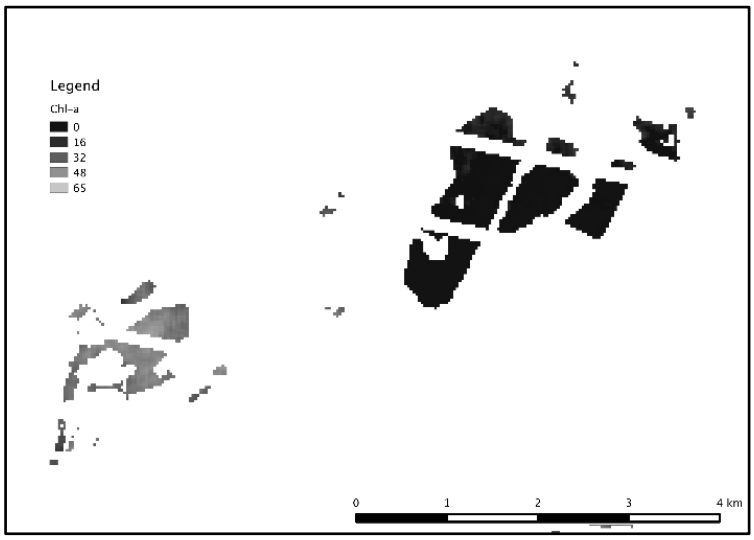

Fig. 6 *Chl-a on Oplatil and Bohdanecsky rybnik on 2012.08.01*

For September 11th, the averages for the two water bodies were 2.8 μg L^{-1} and 39.6 μg L^{-1} (Fig. 7), analysis in September 18th revealed 5.3 and 42.3 (Fig. 8), respectively. Finally, in November 14th, the average Chl-a were 1.9 μg L^{-1} for Oplatil and 27.0 μg L^{-1} for Bohdanecsky rybnik (Fig. 9).

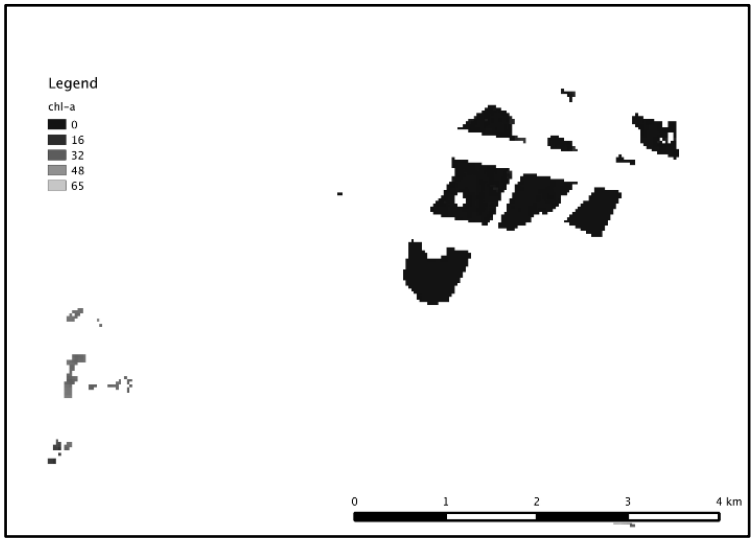

Fig. 7 *Chl-a on Oplatil and Bohdanecsky rybnik on 2012.09.11*

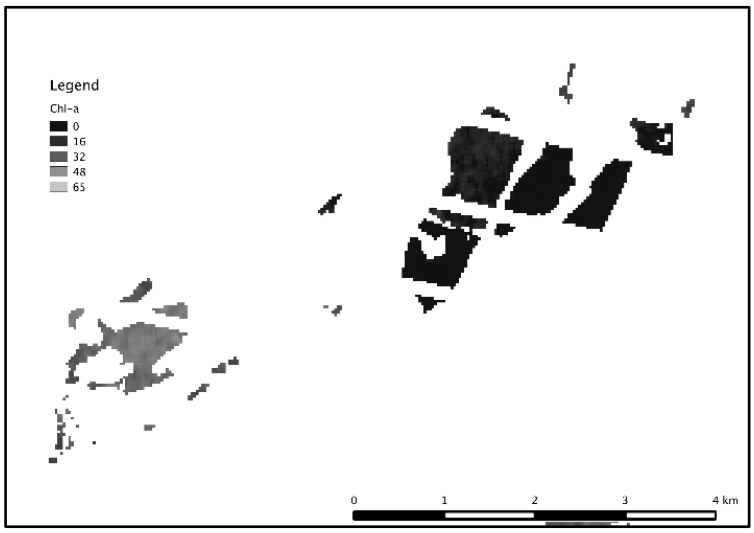

Fig. 8 *Chl-a on Oplatil and Bohdanecsky rybnik on 2012.09.18*

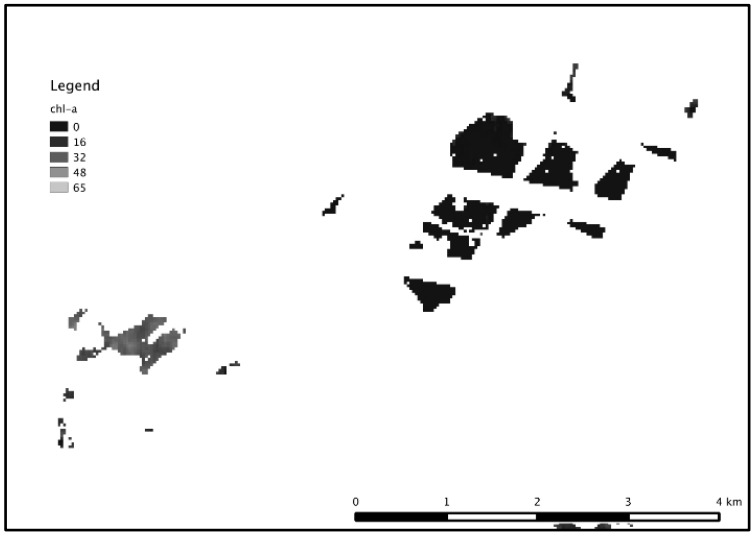

Fig. 9 *Chl-a on Oplatil and Bohdanecsky rybnik on 2012.11.14*

The highest average value for Bohdanecsky rybnik was ascertained in June whereas that one for Oplatil in September, but the general trend in time is quite similar for both water bodies, showing that the algae behave similarly in different water bodies depending on the weather conditions (Fig. 10).

It is possible to apply the models on different water reservoirs that appear on the satellite images and, in the same way, for different water quality parameters.

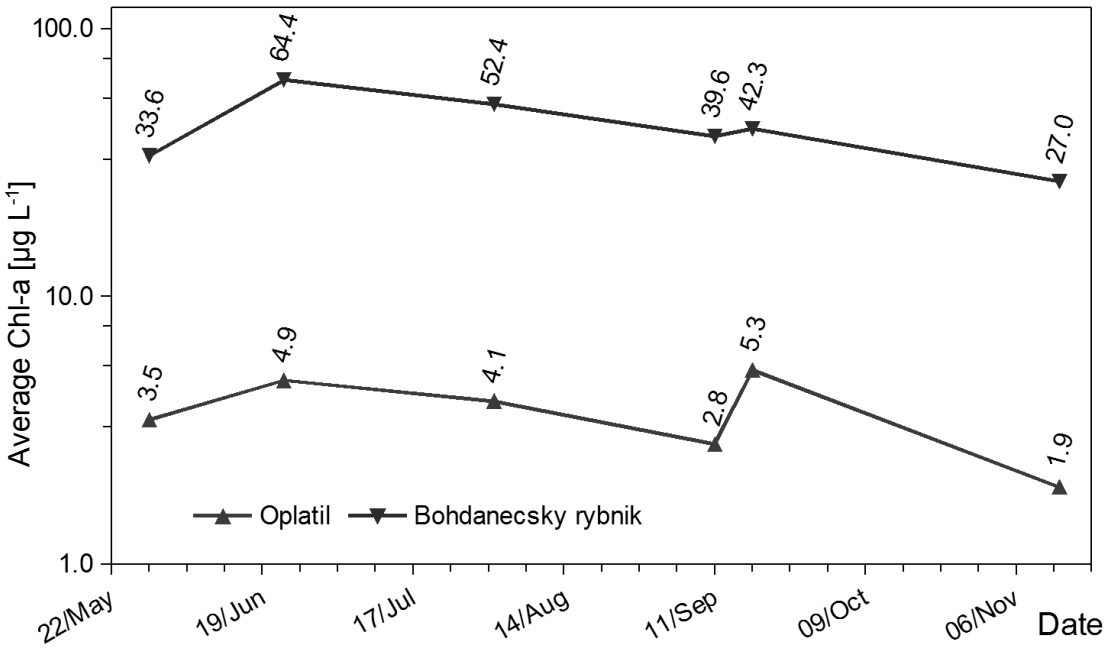

Fig. 10 *Chl-a levels for Bohdanecsky rybnik and Oplatil in 2012 based on model*

Conclusions

Inland water quality monitoring of small water bodies based on the remote sensing looks very promising. From the application of the developed models, it is shown how such a sensing may rely on as a tool for monitoring the quality of inland water reservoirs, especially those that are quite difficult to access or those applicable in simultaneous monitoring of a large number of water bodies which could be hard to achieve using traditional methods. Though being promising, there is a task of covering by haze and cloud shadows, making the use of images often difficult or nearly impossible in the climatic conditions of the Czech Republic. This prolongs the time to gather sufficient data for creating reliable models, but — more importantly —, lowers the reliability of getting the monitored data from the models in uninterrupted regular intervals as it is common with traditional monitoring. This situation would be improved by incorporating other satellites with shorter revisit time.

All the tested water quality parameters can be monitored using satellite remote sensing, although it is also evident that not all is monitored with the same precision enabled by this method. Also, most of the parameters depend on similar band combinations. It suffices to say that the concentrations ascertained with the aid of model parameters will have a strong intercorrelation. In some situations that might not be the case in real situations, such parameters can behave independently. An example is SDD and Chl-a under circumstances of high turbidity not related to algae growth in small inland water bodies.

This paper has proved that the use of Landsat ETM+ in the monitoring on small inland water reservoirs is feasible. With the help of water-only-mask which is adapted when undertaking the smoothing procedure of image processing, it should be possible to monitor even water bodies as small as water objects whose size corresponds to a few pixels at the image.

Acknowledgements

This work was supported by the University of Pardubice (Project No. SGS_2018_003). Authors thank the U.S. Geological Survey for making the Landsat® imagery available for this study. Authors also thank Prof. Jaromíra Chýlková for her help to determine the TC, TOC, and TN in the samples.

References

[1] Mishra D.R., Ogashawara I., Gitelson A.A. (eds.): *Bio-optical modeling and remote sensing of inland waters*. Elsevier, Amsterdam, 2017.

[2] Erdmann E.S., Greb S.S.: Research and monitoring of lake water quality using remote sensing. https://www.uwsp.edu/cnr-ap/UWEXLakes/Documents/programs/Convention/2013/EricErdman-ResearchAndMonitoringOfLakeWaterQualityUsingRemoteSensing.pdf. (accessed May 27, 2018).

[3] Akbar T.A., Hassan Q.A., Achari G.: A remote sensing based framework for predicting water quality of different source waters. *The International Archives of Photogrammetry, Remote Sensing and Spatial Information Sciences* **34** (2010) 1–4.

[4] Novoa S., Chust G., Valencia V., Froidefond J.-M., Morichon D.: Estimation of chlorophyll-a concentration in waters over the continental shelf of the Bay of Biscay: A comparison of remote sensing algorithms. *International Journal of Remote Sensing* **32** (2011) 8349–8371.

[5] Sun D., Qiu Z., Li Y., Shi K., Gong S.: Detection of total phosphorus concentrations of turbid inland waters using a remote sensing method. *Water, Air, & Soil Pollution* **225** (2014) 1953.

[6] Rundquist D.C., Han L., Schalles J.F., Peake J.S.: Remote measurement of algal chlorophyll in surface waters: The case for the first derivative of reflectance near 690 nm, *Photogrammetric Engineering and Remote Sensing* **62** (1996) 195–200.

[7] Harding L.W., Itsweire E.C., Esaias W.E.: Algorithm development for recovering chlorophyll concentrations in the Chesapeake Bay using aircraft remote sensing, 1989–91. *Photogrammetric Engineering and Remote Sensing* **61** (1995) 177–185.

[8] Lesht B., Barbiero R.P., Warren G.J.: A band-ratio algorithm for retrieving open-lake chlorophyll values from satellite observations of the Great Lakes. *Journal of Great Lakes Research*. **39** (2013) 138–152.

[9] Dekker G.A., Hestir E.L.: *Evaluating the feasibility of systematic inland water quality monitoring with satellite remote sensing*, CSIRO, Canberra 2012.

[10] Malthus T.J., Hestir E.L., Dekker A.G., Brando V.E.: The case for a global inland water quality product, in: *Geoscience and Remote Sensing Symposium (IGARSS), 2012 IEEE International*. IEEE, Munich 2012: pp. 5234–5237.

[11] Hellweger F.L., Schlosser P., Lall U., Weissel J.K.: Use of satellite imagery for water quality studies in New York Harbor. *Estuarine, Coastal and Shelf Science* **61** (2004) 437–448.

[12] Sudheer K.P., Chaubey I., Garg V.: Lake water quality assessment from Landsat Thematic Mapper data using neutral network: An approach to optimal band combination selection. *Journal of The American Water Resources Association* **42** (2006) 1683–1695.

[13] Papoutsa C., Hadjimitsis D.G.: Remote Sensing for Water Quality Surveillance in Inland Waters: The Case Study of Asprokremmos Dam in Cyprus, in: Hadjimitsis D.G. (Ed.): *Remote Sensing of Environment: Integrated Approaches*. IntechOpen, London 2013, pp. 131–152.

[14] Shi K., Li Y., Li L., Lu H., Song K., Liu Z., Xu Y., Li Z.: Remote chlorophyll-a estimates for inland waters based on a cluster-based classification. *Science of The Total Environment* **444** (2013) 1–15.

[15] Wang Y., Xia H., Fu J., Sheng G.: Water quality change in reservoirs of Shenzhen, China: detection using LANDSAT/TM data. *Science of The Total Environment* **328** (2004) 195–206.

[16] Brezonik P., Menken K.D., Bauer M.: Landsat-based remote sensing of lake water quality characteristics, including chlorophyll and colored dissolved organic matter (CDOM). *Lake and Reservoir Management* **21** (2005) 373–382.

[17] Braga C.Z.F., Setzer A.W., Drude de Lacerda L.: Water quality assessment with simultaneous Landsat-5 TM data at Guanabara Bay, Rio de Janeiro, Brazil. *Remote Sensing Environment* **45** (1993) 95–106.

[18] Mayo M., Gitelson A., Yacobi Y.Z., Ben-Avraham Z.: Chlorophyll distribution in lake Kinneret determined from Landsat Thematic Mapper data. *Remote Sensing* **16** (1995) 175–182.

[19] Hadjimitsis D.G., Clayton C.R.I., Hope V.S.: An assessment of the effectiveness of atmospheric correction algorithms through the remote sensing of some reservoirs. *International Journal of Remote Sensing* **25** (2004) 3651–3674.

[20] Wang F., Qin Z., Song C., Tu L., Karnieli A., Zhao S.: An improved mono-window algorithm for land surface temperature retrieval from Landsat 8 thermal infrared sensor data. *Remote Sensing* **7** (2015) 4268–4289.

[21] Schneider K., Mauser W.: Processing and accuracy of Landsat Thematic Mapper data for lake surface temperature measurement. *International Journal of Remote Sensing* **17** (1996) 2027–2041.

[22] Kukla P.: Analýza historického vývoje krajiny se zvláštním zřetelem na vodní složku krajiny (Analysis of historical development of landscape with special regard to water component), in: *Venkovská Krajina 2007. Sborník z 5. ročníku mezinárodní mezioborové conference.* Česká společnost pro krajinnou ekologii, Hostěnín 2007: pp. 71–76.

[23] Robinson I.S.: Measuring the ocean from space: The principles and methods of satellite oceanography. Springer Science and Business Media, Heidelberg 2004.

[24] Olmanson L.G., Bauer M.E., Brezonik P.L.: A 20-year Landsat water clarity census of Minnesota's 10,000 lakes. *Remote Sensing of Environment* **112** (2008) 4086–4097.

[25] Kloiber S.M., Brezonik P.L., Olmanson G.L., Bauer M.E.: A procedure for regional lake water clarity assessment using Landsat multispectral data. *Remote Sensing Environment* **82** (2002) 38–47.

[26] Czech Normalization Institute: ČSN ISO 10260: Spektrofotometrické stanovení koncentrace chlorofylu-a (Spectrometric determination of the chlorophyll-a concentration), CNI, Prague 1995.

[27] Adrefouet S., Bindschandler R., Brown de Colstoun E., Choate M., Chomentowski W., Christopherson J., Doom B., Hall D.K., Holifield C., Howard S., Kranenburg C., Lee S., Masek J.G., Moran M.S., Mueller-Karger F., Ohlen D., Palandro D., Price J., Qi J., Reed B., Samek J., Scaramuzza P., Skole D., Schott J., Storey J., Thome K., Torres-Pilliza D., Vogelmann J., Williams D., Woodcock C., Wylie B.: *Preliminary assessment of the value of Landsat 7 ETM+ data following scan line corrector malfunction*. United States Geological Survey, Sioux Falls 2003.

[28] Landsat 7 data users handbook. https://landsat.usgs.gov/landsat-7-data-users-handbook. (accessed May 27, 2018).

[29] Gonzalez R.C., Woods R.E.: *Digital image processing, 2nd Ed*. Prentice Hall, New Jersey 2002.

[30] Bonansea M., Rodriguez M.C., Pinotti L., Ferrero S.: Using multi-temporal Landsat imagery and linear mixed models for assessing water quality parameters in Río Tercero reservoir (Argentina). *Remote Sensing of Environment* **158** (2015) 28–41.

[31] Smith L.C., Pavelsky T.M.: Remote sensing of volumetric storage changes in lakes. *Earth Surface Landforms* **34** (2009) 1353–1358.